

We are IntechOpen, the world's leading publisher of Open Access books Built by scientists, for scientists

4,900

Open access books available

124,000

International authors and editors

140M

Downloads

Our authors are among the

154

Countries delivered to

TOP 1%

most cited scientists

12.2%

Contributors from top 500 universities



WEB OF SCIENCE™

Selection of our books indexed in the Book Citation Index
in Web of Science™ Core Collection (BKCI)

Interested in publishing with us?
Contact book.department@intechopen.com

Numbers displayed above are based on latest data collected.
For more information visit www.intechopen.com



Structural Instability of Carbon Nanotube

I-Ling Chang
National Cheng Kung University
Taiwan

1. Introduction

Since Iijima reported MWCNTs in 1991, CNTs have captured the intensive attention of researchers worldwide due to the combination of their expected structural perfection, small size, low density, high stiffness, high strength, and excellent electronic properties. CNTs have been widely adopted as microscopic probing tips (Dai et al., 1996; Hafner et al., 2001), nanocomposites reinforcements (Bower et al., 1998; Jin et al., 1998), nanotweezers (Kim & Lieber, 1999), and nanoactuators (Baughman et al., 1999; Fennimore et al., 2003) due to their slender and high aspect ratio structures. Meanwhile, nanotubes are also highly susceptible to buckling under compression, which is a structural instability. Once the buckling of CNTs occurs, the load-carrying capability would suddenly reduce and lead to possible catastrophic failure of the nanotubes, which significantly limit the loading strengths of the probing tips and compressive strengths of nanocomposite structures. Even the physical properties such as conductance of carbon nanotube can be influenced by the occurrence of buckling (Postma et al., 2001). Hence, it is crucial to understand the mechanism of nanotube buckling and even predict the onset of buckling in order to improve the nanotube applications.

A review of the relevant literature shows that significant studies have employed both experimental (Falvo et al., 1997; Iijima et al., 1996; Thostenson & Chou, 2004; Waters et al., 2004) and theoretical (Ru, 2000; Yakobson & Avouris, 2001) approaches to investigate the buckling behaviors of CNTs. However due to the difficulties encountered at nanoscale, the experimental investigation of the buckling behaviors of CNTs remains a challenging problem and individual factors that affect buckling could not be easily identified. In theoretical study, the CNTs are commonly treated as beams or thin-shell tubes with certain wall thickness and elastic constants and, thus, it is difficult to consider the chirality and size effects on buckling behavior of CNTs because the continuum assumption disregards the discrete nature of atomic structures (Ru, 2000; Yakobson & Avouris, 2001). Some researchers attempted to introduce the atomic-continuum method combining the atomic detail in the continuum description and examine the various properties of CNTs (Chang, 2004; Guo et al., 2008; Li & Chou, 2003a, 2003b). The atomic-continuum method could shorten the computational time in larger atomic system.

As the fast development and rapid advancement of computers, molecular approaches have become important tools and are widely applied to study the factors that would influence the buckling of CNTs (Buehler et al., 2004; Cao & Chen, 2006a, 2006b; Huh & Huh, 2008; Liew et al., 2004; Ozaki et al., 2000). Although some researchers already discussed various aspects of

the CNT buckling behavior, systematic analysis on the effect of geometry (i.e. radius, length and length-to-radius ratio) and chirality (i.e. armchair, zigzag and chiral) on the buckling mechanism is still lacking to the best of our knowledge. Consequently, the present study employs MD simulations based on the Tersoff many-body potential function (Tersoff, 1986, 1988, 1989) to perform a systematic and comprehensive investigation into the buckling behaviors of single-walled CNTs under uniaxial compressive displacement loading. Besides, the applicability of the continuum buckling theory, which has been well developed for thin tubes, on predicting the buckling behavior of the CNT will also be examined.

2. Methodology

Atomic model of the single-walled CNT with radius r and axial length L are illustrated in Fig. 1. All simulations are performed at room temperatures, 300K using a rescaling method and Newton's equations of motion are solved using a fifth order Gear's predictor-corrector algorithm. The empirical Tersoff many-body potential (Tersoff, 1986, 1988, 1989), which is commonly adopted in CNTs molecular simulation studies to provide quick estimation and significant insight into the thermo-mechanical behavior, is employed to describe the interatomic interaction between the carbon atoms. The force acting on an individual atom is obtained by summing the forces contributed by the surrounding atoms. The initial atomic models of CNT will be relaxed under NTP ensemble for 10000 time steps with a 1 fs step size to make sure the nanotubes reach their equilibrium states.

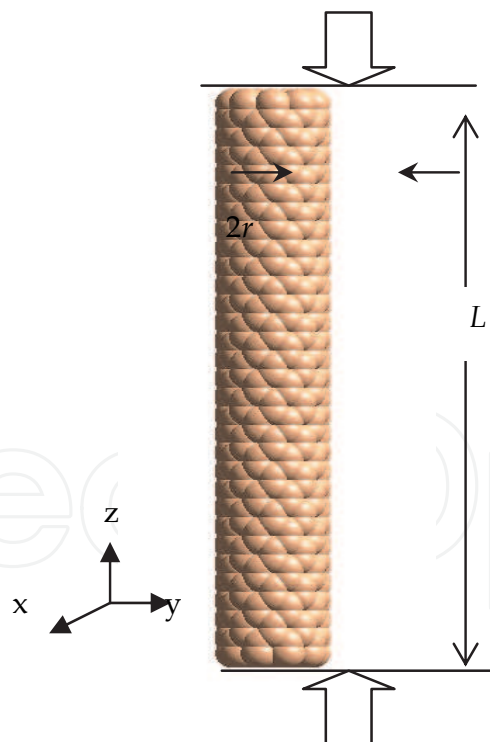


Fig. 1. The schematic presentation of the CNT under uniaxial compression.

During the simulations, the nanotube is compressed uniaxially and incrementally along z direction by a uniform strain under NTV ensemble. The periodic boundary condition (PBC) is applied in the axial direction, which served as a loading mechanism to apply uniform displacements. Minimum image criterion is adopted to implement the periodic boundary

condition. In order to reduce the loading strain rate, additional MD steps are applied for the relaxation of the CNT after each stage of the compression. The equilibrated configuration will be used as the initial state for the next loading step. In this study, the applied strain increment is 0.5%, then the CNT atomic system is relaxed for the interval of 10 *ps* and the corresponding strain rate is 0.05% *ps*⁻¹. The total energy, pressure and atomic configuration of the relaxed structure are monitored at each loading step to determine whether the buckling of the CNT occurs. Once a sudden jump in the total energy, as illustrated in Fig. 2, is observed, the atomic configuration of the nanotube would be inspected. Buckling strains (or called critical compressive strains) can be indicated from the jumps in the total energy and pressure.

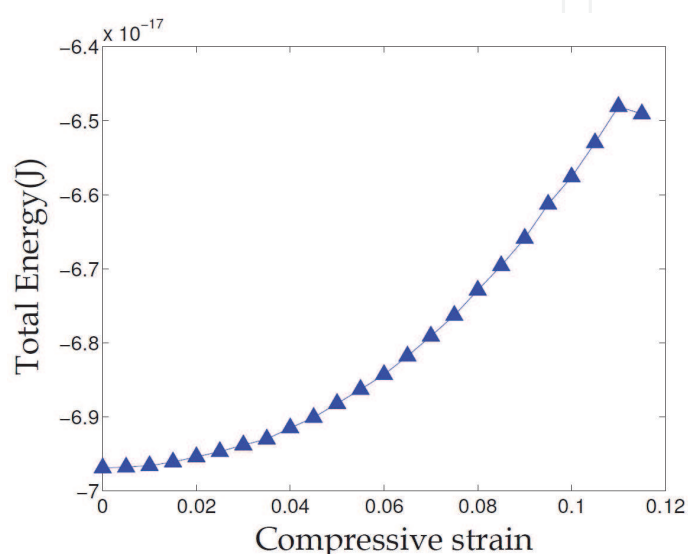


Fig. 2. The relation between the system energies and compressive strains for (5,5) CNT with length of 7.38Å.

CNTs can be considered as a graphene sheet rolled into a cylindrical shell and three distinct types of nanotubes could be classified as armchair, zigzag and chiral according to the way of rolling-up. In order to assess the influence of geometry and chirality on the buckling behavior of the single-walled CNTs, various radii, lengths, length-to-radius ratios and helical types of CNTs would be simulated and elucidate the dependence of buckling strain.

The length-to-radius ratio (or called slenderness ratio) is defined as $S.R. = \frac{L}{r}$. The radius and translation length, which is the smallest periodic axial distance, of (*m,n*) CNTs can be calculated as

$$r = \frac{a\sqrt{3(n^2 + m^2 + mn)}}{2\pi}$$

$$T_{(m,n)} = 2\pi r \frac{\sqrt{3}}{d_R}$$

where *a* is the interatomic C-C bond length, 1.42Å and *d_R* is the greatest common divisor of 2*n* + *m* and 2*m* + *n*. Since the periodic boundary condition is employed as a loading

mechanism, the simulated CNT length must be multiple of the translation length so that the complete six-membered ring structure of the CNT could be preserved. The geometric parameters, radius r and length L , for different chiralities of CNTs are listed in Table 1-3, respectively. Similar radius, length and slenderness ratio for armchair, zigzag and chiral CNTs are chosen, if possible, for the simulation. Since the translation lengths for (6,4), (9,6) and (12,8) chiral CNTs are 18.569 Å, the choices of slenderness ratios for chiral CNTs are more limited.

(m,n)	(5,5)	(8,8)	(10,10)
Radius(Å)	3.39	5.424	6.78
Length(Å) / S.R.	7.38 / 2.18	12.3 / 2.27	14.76 / 2.18
	12.30 / 3.63	19.68 / 3.63	24.595 / 3.63
	36.89 / 10.88	59.03 / 10.88	73.79 / 10.88
	61.49 / 18.14	98.38 / 18.14	122.98 / 18.14
	86.08 / 25.39	137.73 / 25.39	172.165 / 25.39
	147.57 / 43.53	236.11 / 43.53	295.14 / 43.53

Table 1. The radii and lengths of the modeled armchair CNTs

(m,n)	(9,0)	(14,0)	(17,0)
Radius(Å)	3.523	5.48	6.655
Length(Å) / S.R.	8.52 / 2.42	12.78 / 2.33	17.04 / 2.56
	12.78 / 3.63	21.3 / 3.89	25.56 / 3.84
	38.34 / 10.88	59.64 / 10.88	72.42 / 10.88
	63.9 / 18.14	97.98 / 17.88	119.28 / 17.92
	89.46 / 25.39	140.58 / 25.65	170.4 / 25.60
	153.36 / 43.53	238.56 / 43.53	289.68 / 43.53

Table 2. The radii and lengths of the modeled zigzag CNTs

(m,n)	(6,4)	(9,6)	(12,8)
Radius(Å)	3.413	5.119	6.825
Length(Å) / S.R.	18.569 / 5.44	18.569 / 3.62	18.569 / 2.72
	37.138 / 10.88	55.707 / 10.88	74.276 / 10.88
	55.707 / 16.32	92.845 / 18.14	129.982 / 18.92
	92.845 / 27.20	129.982 / 25.39	167.712 / 24.57
	148.55 / 43.52	222.83 / 43.53	297.10 / 43.53

Table 3. The radii and lengths of the modeled chiral CNTs

3. Results

MD approaches are utilized to simulate the uniaxial compression test of CNTs with different geometries and chiralities. The size and chirality effects on buckling behaviors are studied and systematically compared through the critical compressive strains. It is noticed that two distinct types of buckling configurations are commonly observed as shown in Fig. 3 (a) and (b). One is shell wall buckling with kinks on the wall with the tube's centerline remaining

straight, which is a local instability and the other is column buckling, which buckle as a whole. Moreover, there is another intriguing type of initial buckling configuration, which starts with a bump on the wall as shown in Fig. 3(c), and the CNT will eventually turn into column or shell wall buckling. It is also observed that the buckling kinks or bends appear mostly near the middle of the nanotubes, which indicates the loading mechanism does not impose any extra constraint on the two ends. Unlike the velocity controlled loading (Jeng et al, 2004), the drastic deformation starts from the imminent places near the ends due to Poisson's effect. Hence, it is difficult to separate the boundary constraint effect from the other investigating factors. It is also noted that the radial distribution function before and after buckling is quite similar as shown in Fig. 4, which implies that the bond structures do not change due to buckling.

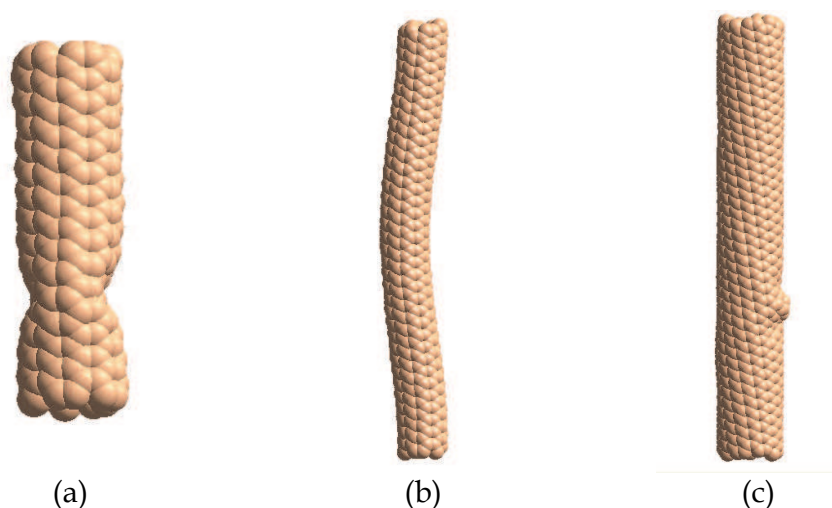


Fig. 3. The buckled shapes of CNTs. (a) shell wall, (b) column and (c) bump on the wall.

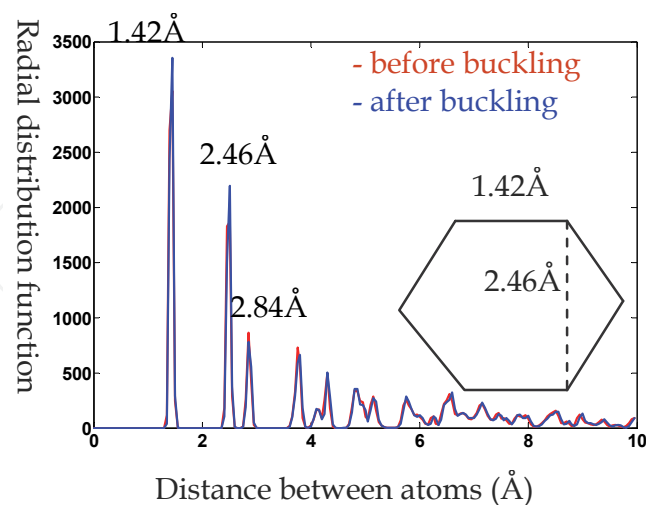


Fig. 4. The radial distribution functions before and after buckling.

The buckling strains for different chirality and slenderness ratio of CNTs are shown in Fig. 5, 6 and 7, respectively. The filled marks indicate column buckling and the empty one indicate shell wall buckling. In general, the nanotube's buckling behavior transits from shell

wall type for a short tube to column type for a long tube of the same radius irrespective to the chirality of the CNTs. For slender nanotubes ($S.R. \geq 20$), axial compression results in “global buckling” while the nanotubes undergo “local buckling” for stout nanotubes ($S.R. \leq 10$). It is noticed that the slenderness ratio has strong influence on the buckling strains and the buckling strains decrease rapidly with the increase of slenderness ratio particularly for CNTs with smaller radii. Under similar length-to-radius ratio, it is noted that the buckling strain decreases as the radius of the CNT increases especially for CNTs with smaller slenderness ratios. It is observed that the chirality of the CNTs does not affect the buckling behaviors and buckling strains significantly.

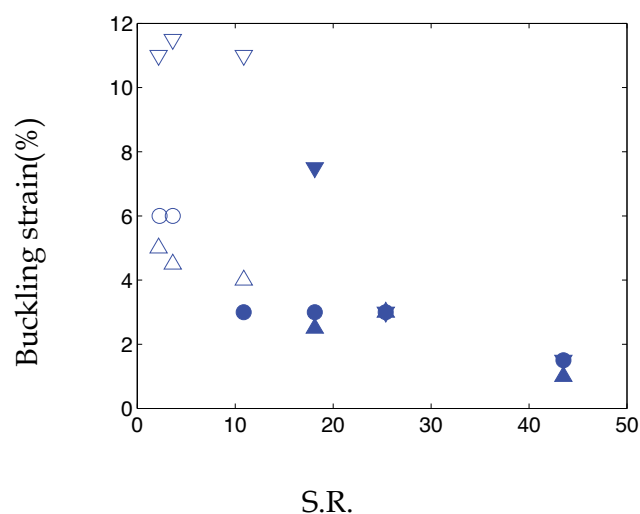


Fig. 5. The relationship between the buckling strain and slenderness ratio for armchair CNTs. $\nabla\nabla$: (5,5), $\circ\bullet$: (8,8), $\triangle\blacktriangle$: (10,10) CNT.

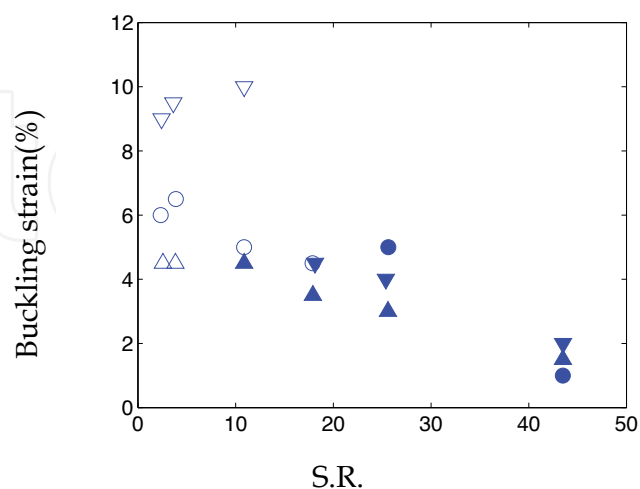


Fig. 6. The relationship between the buckling strain and slenderness ratio for zigzag CNTs. $\nabla\nabla$: (9,0), $\circ\bullet$: (14,0), $\triangle\blacktriangle$: (17,0) CNT.

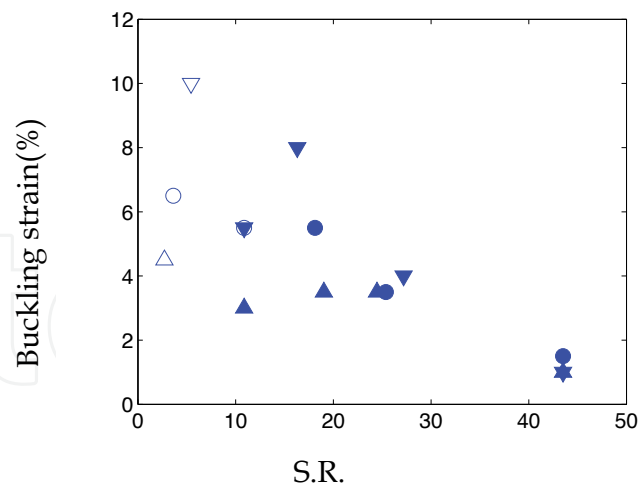


Fig. 7. The relationship between the buckling strain and slenderness ratio for chiral CNTs. ∇ : (6,4), \circ : (9,6), \triangle : (12,8) CNT.

4. Analysis and discussion

From current simulation results, it is very difficult to deduce a clear relationship between the critical compressive buckling strain and the CNT geometry and helical type, not to mention predicting the buckling type. In continuum mechanics, there already exist theories to calculate the buckling strain of thin shell tube depending on the buckling type in macroscopic scale. However, the applicability of continuum buckling theory in nanoscale is still an unsolved question. Hence, the continuum predictions on the buckling strains and the simulation results will be compared in order to examine the applicability.

By using Euler-Bernoulli beam theory, the critical buckling strain of a tube with both ends clamped displaying the column-like buckling behavior can be described as (Landau et al., 1986)

$$\epsilon_{cr}^{column} = \frac{\pi^2 \left[\left(r + \frac{t}{2} \right)^2 - \left(r - \frac{t}{2} \right)^2 \right]}{L^2} \quad (1)$$

where t is the thickness of the tube. If $t \ll r$, the equation could be rewritten as

$$\epsilon_{cr}^{column} = 2 \left(\frac{\pi r}{L} \right)^2 \quad (2)$$

It is noticed that the critical compressive buckling strain decreases as the inverse square of the slenderness ratio for column-type buckling. On the other hand, the critical compressive buckling strain of the tube displaying the shell-like buckling behavior is (Libai & Simmonds, 1998; Timoshenko & Gere, 1961)

$$\epsilon_{cr}^{shell} = \frac{1}{\sqrt{3(1-\nu^2)}} \frac{t}{r} \approx 0.588 \frac{t}{r} \quad (3)$$

The Poisson's ratio, ν , of the CNTs is chosen as 0.19 (Yakobson et al. 1996). It is noted that the critical compressive strain of shell-like buckling depends only on the tube thickness and radius, but is independent of the tube length.

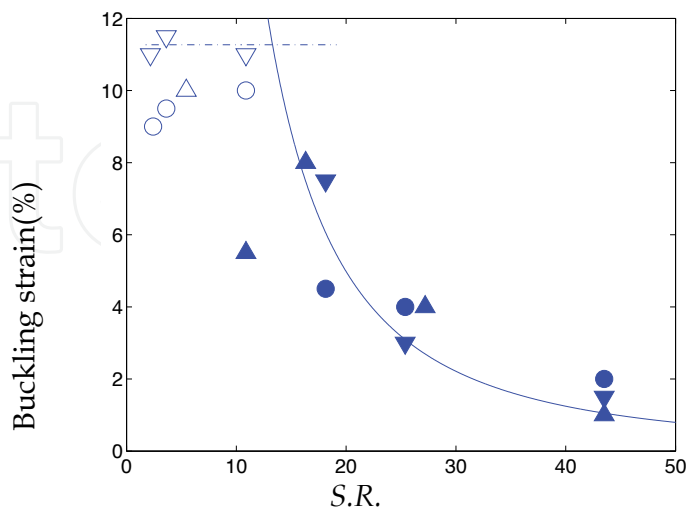


Fig. 8. The comparisons between the continuum predictions and molecular simulation results for CNTs. ▽▼:(5,5), ○●:(9,0) and △▲:(6,4)

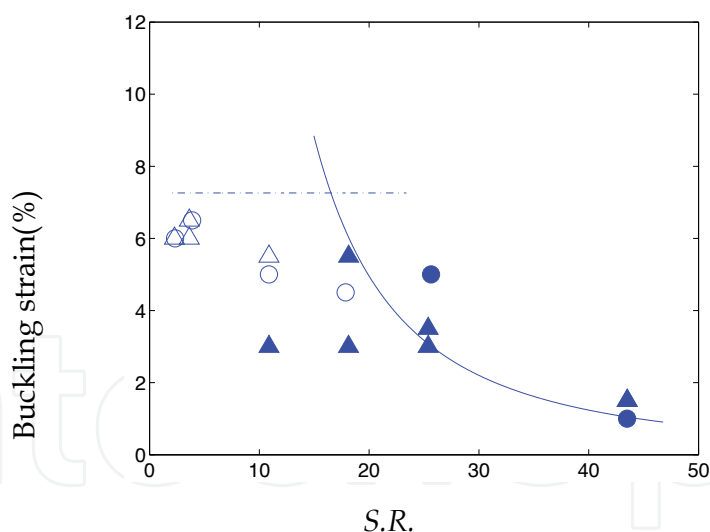


Fig. 9. The comparisons between the continuum predictions and molecular simulation results for CNTs. ▽▼:(8,8), ○●:(14,0) and △▲:(9,6)

Fig. 8, 9 and 10 illustrate the comparisons between the continuum predictions on the buckling strains and the simulation results for respective set of similar radii. One of the uncertainties of the continuum model is the effective nanotube thickness. Here in this research, the effective nanotube thickness is chosen as 0.66\AA (Yakobson et al. 1996), which is roughly the atomic radius of carbon, instead of the commonly used CNT wall thickness, 3.4\AA . Since the nanotube thickness is not negligible as compared to the radius, Eq. (1) is

adopted in the comparison. The dash lines illustrate the continuum prediction of shell-like buckling while the solid lines depict the prediction based on Euler-Bernoulli beam theory. It is observed that the buckling resistance does not show obvious dependence on the CNT chirality under similar radii. The continuum prediction of shell-like buckling can serve as an upper bound for predicting the shell wall buckling but significantly overestimate the buckling strains for nanotubes with higher length-to-radius ratio irrespective to the nanotube chirality. As the slenderness ratio becomes higher, the continuum prediction based on Euler-Bernoulli beam theory could capture the trend of column type buckling but also overestimate the buckling strains for nanotubes with smaller length-to-radius ratio. It is observed that those buckling strain which deviate significantly from the continuum prediction are at the intersection region of the two continuum theories. It is speculated that the difference in buckling strain between the continuum theories and simulation results at the transition region could be due to the competition between two buckling mechanisms.

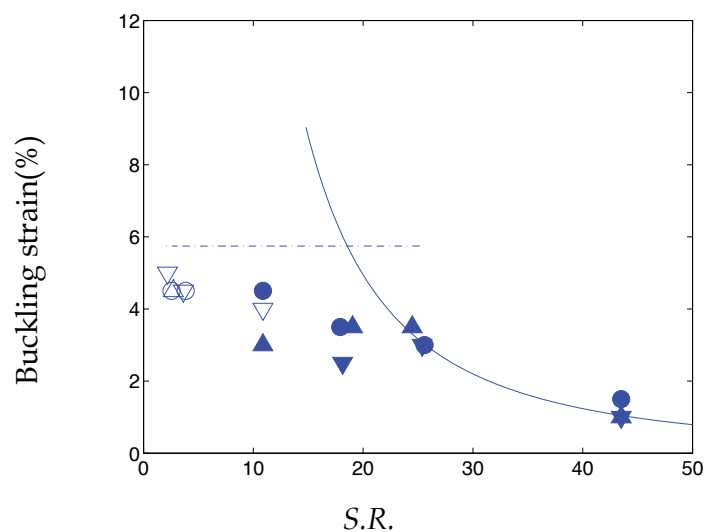


Fig. 10. The comparisons between the continuum predictions and molecular simulation results for CNTs. ∇ \blacktriangledown : (10,10), \circ \bullet : (17,0) and \triangle \blacktriangle : (12,8)

5. Conclusion

In this work, molecular dynamics approach is employed to study the buckling behaviors of single-walled carbon nanotubes with different geometric sizes and chiralities under room temperature. Based on the MD simulation results, it is observed that the nanotube's buckling behavior transits from shell wall type for a short tube to column type for a long tube of the same radius irrespective to the chirality of the CNTs. Moreover, the buckling strain is getting smaller as the CNT becomes slender for most nanotubes, which implies that the slender nanotubes have lower buckling resistance. Under similar length-to-radius ratio, it is noted that the buckling strain decreases as the radius of the CNT increases especially for CNTs with smaller slenderness ratios. From the comparison with the prediction made by continuum buckling theories, it is concluded that the corresponding buckling strain and buckling type predicted by the continuum theory could agree reasonably well with MD simulations of the CNTs under compression except at the transition region. From the findings of this paper, it is suggested that the continuum buckling theory with proper choice of parameters, i.e., wall thickness and Poisson's ratio, could capture the trend of the

buckling strain on the length-to-radius ratio disregarding to the helical types (i.e., armchair, zigzag and chiral) of the nanotubes and, hence, could serve as a primitive guideline in predicting the buckling strain of the CNTs.

6. Acknowledgment

This research work is supported by National Science Council of Taiwan under the grants NSC97-2221-E-194-015 and NSC98-2221-E-194-012-MY2. The support of AFOSR under Contract No. FA2386-09-1-4152 AOARD 094152 is also acknowledged. We are also grateful to the Taiwan National Center for High-performance Computing for computer time and facilities.

7. Reference

- Baughman, R. H.; Cui, C. X.; Zakhidov, A. A.; Iqbal, Z.; Barisci, J. N.; Spinks, G. M.; Wallace, G. G.; Mazzoldi, A.; De Rossi, D.; Rinzler, A. G.; Jaschinski, O.; Roth, S. & Kertesz, M. (1999). Carbon Nanotube Actuators, *Science*, Vol.284, No.5418, (May 1999), pp.1340-1344, ISSN 0036-8075
- Bower, C.; Rosen, R.; Jin, L.; Han J. & Zhou, O. (1999). Deformation of Carbon Nanotubes in Nanotube-Polymer Composites, *Applied Physics Letters*, Vol.74, No. 22, (May 1999), pp.3317-3319, ISSN 0003-6951
- Buehler, M.; Kong, Y. & Gao, H. (2004). Deformation Mechanisms of Very Long Single-Wall Carbon Nanotubes Subject to Compressive Loading, *Journal of Engineering Materials and Technology*, Vol.126, No.3, (July 2004), pp.245-249, ISSN 0094-4289
- Cao, G. & Chen, X. (2006a). Mechanisms of Nanoindentation on Single-Walled Carbon Nanotubes: The Effect of Nanotube Length, *Journal of Materials Research*, Vol.21, No. 4, (April 2006), pp.1048-1070, ISSN 0884-2914
- Cao, G. & Chen, X. (2006b). Buckling Behavior of Single-walled Carbon Nanotubes and a Targeted Molecular Mechanics Approach, *Physical Review B*, Vol.73, No.16, (October 2006), pp.155435, ISSN 1098-0121
- Chang, T. (2004). Buckling of Single-Walled Carbon Nanotubes via a Hybrid Atomic/Continuum Approach, *Acta Mechanica Sinica*, Vol.36, No.6, (November 2004), pp.744-748,
- Dai, H.; Hafner, J. H.; Rinzler, A. G.; Colbert, D. T. & Smalley, R. E. (1996). Nanotubes as Nanoprobes in Scanning Probe Microscopy, *Nature*, Vol.384, No.6605, (November 1996), pp.147-150, ISSN 0028-0836
- Falvo, M. R.; Clary, G. J.; Taylor, R. M.; Chi, V.; Brooks, F. P.; Washburn, S. & Superfine, R. (1997). Bending and Buckling of Carbon Nanotubes under Large Strain, *Nature*, Vol.389, No. 6651, (October 1997), pp.582-584, ISSN 0028-0836
- Fennimore, A. M.; Yuzvinsky, T. D.; Han, W. Q.; Fuhrer, M. S.; Cumings, J. & Zettl, A. (2003). Rotational Actuators based on Carbon Nanotubes, *Nature*, Vol.424, No.6947, (July 2003), pp. 408-410, ISSN 0028-0836
- Guo, X.; Leung, A.Y.T.; He, X.Q.; Jiang H. & Huang Y. (2008). Bending Buckling of Single-Walled Carbon Nanotubes by Atomic-Scale Finite Element, *Composites Part B-Engineering*, Vol.39, No.1, pp.202-208, ISSN 1359-8368

- Hafner, J. H.; Cheung, C. L.; Woolley A. T. & Lieber, C. M. (2001). Structural and Functional Imaging with Carbon Nanotube AFM Probes, *Progress in Biophysics & Molecular Biology*, Vol.77, No.1, pp.73-110, ISSN 0079-6107
- Huh, J. & Huh H. (2008). Effect of Helicity on the Buckling Behavior of Single-Wall Carbon Nanotubes, *International Journal of Modern Physics B*, Vol.22, No.31-32, (December 2008), pp.5872-5877, ISSN 0217-9792
- Iijima, S.; Brabec, C.; Maiti, A. & Bernholc, J. (1996). Structural Flexibility of Carbon Nanotubes, *Journal of Chemical Physics*, Vol.104, No.5, (February 1996), pp.2089-2092, ISSN 0021-9606
- Jeng, Y.-R.; Tsai, P.-C. & Fang, T.-H. (2004). Effects of Temperature and Vacancy Defects on Tensile Deformation of Single-Walled Carbon Nanotubes, *Journal of Physics and Chemistry of Solids*, Vol.65, No.11, (November 2004), pp.1849-1856, ISSN 0022-3697
- Jin, L.; Bower, C. & Zhou, O. (1998). Alignment of Carbon Nanotubes in a Polymer Matrix by Mechanical Stretching, *Applied Physics Letters*, Vol.73, No.9, (August 1998), pp.1197-1199, ISSN 0003-6951
- Kim, P. & Lieber, C. M. (1999). Nanotube Nanotweezers, *Science*, Vol.286, No.5447, (December 1999), pp.2148-2150, ISSN 0036-8075
- Landau, L. D.; Pitaevskii, L. P.; Lifshitz, E. M. & Kosevich, A. M. (1986). *Theory of Elasticity*, Butterworth-Heinemann, ISBN 978-075-0626-33-0, Oxford, UK
- Li, C & Chou, T.-W. (2003a). A Structural Mechanics Approach for the Analysis of Carbon Nanotubes, *International Journal of Solids and Structures*, Vol.40, No.10, (May 2003), pp. 2487-2499, ISSN 0020-7683
- Li, C & Chou, T.-W. (2003b). Single-Walled Carbon Nanotubes as Ultrahigh Frequency Nanomechanical Resonators, *Physical Review B*, Vol.68, No.7, (August 2003), pp.073405, ISSN 1098-0121
- Libai, A. & Simmonds, J. G. (2005). *The Nonlinear Theory of Elastic Shells*, Cambridge University Press, ISBN 978-052-1019-76-7, Cambridge, UK
- Liew, K. M.; Wong, C. H.; He, X. Q.; Tan, M. J. & Meguid, S. A. (2004). Nanomechanics of Single and Multiwalled Carbon Nanotubes, *Physical Review B*, Vol.69, No.11, (March 2004), pp.115429, ISSN 1098-0121
- Ozaki, T.; Iwasa, Y. & Mitani, T. (2000). Stiffness of Single-Walled Carbon Nanotubes under Large Strain, *Physical Review Letters*, Vol.84, No.8, (February 2000), pp.1712-1715, ISSN 0031-9007
- Postma, H. W. C.; Teepen, T.; Yao, Z.; Grigoni, M. & Dekker, C. (2001). Carbon Nanotube Single-Electron Transistors at Room Temperature, *Science*, Vol.293, No.5527, (July 2001), pp.76-79, ISSN 0036-8075
- Ru, C. Q. (2000). Effective Bending Stiffness of Carbon Nanotubes, *Physical Review B*, Vol.62, No.15, (October 2000), pp.9973-9976, ISSN 0163-1829
- Tersoff, J. (1986). New Empirical-Model for the Structural-Properties of Silicon, *Physical Review Letters*, Vol.56, No.6, (February 1986), pp.632-635, ISSN 0031-9007
- Tersoff, J. (1988). New Empirical-Approach for the Structure and Energy of Covalent Systems, *Physical Review B*, Vol.37, No.12, (April 1988), pp.6991-7000, ISSN 0163-1829
- Tersoff, J. (1989). Modeling Solid-State Chemistry-Interatomic Potentials for Multicomponent Systems, *Physical Review B*, Vol.39, No.8, (March 1989), pp.5566-5568, ISSN 1098-0121

- Thostenson, E. T. & Chou, T.-W. (2004). Nanotube Buckling in Aligned Multi-Wall Carbon Nanotube Composites, *Carbon*, Vol.42, No.14, pp.3015-3018, ISSN 0008-6223
- Timoshenko, S. P. & Gere, J. M. (1961). *Theory of Elastic Stability*, McGraw-Hill, ISBN 978-048-6472-07-2, New York, USA
- Waters, J. F.; Riester, L.; Jouzi, M.; Guduru, P. R. & Xu, J. M. (2004). Buckling Instabilities in Multiwalled Carbon Nanotubes under Uniaxial Compression, *Applied Physics Letters*, Vol.85, No.10, (September 2004), pp.1787-1789, ISSN 0003-6951
- Yakobson, B. I. & Avouris, P. (2001). Mechanical Properties of Carbon Nanotubes, *Topics in Applied Physics*, Vol.80, pp.287-327, ISSN 0303-4216
- Yakobson, B. I.; Brabec, C. J. & Bernholc, J. (1996). Nanomechanics of Carbon Tubes: Instabilities beyond Linear Response, *Physical Review Letters*, Vol.76, No.14, (April 1996), pp.2511-2514, ISSN 0031-9007

IntechOpen



Carbon Nanotubes - Synthesis, Characterization, Applications

Edited by Dr. Siva Yellampalli

ISBN 978-953-307-497-9

Hard cover, 514 pages

Publisher InTech

Published online 20, July, 2011

Published in print edition July, 2011

Carbon nanotubes are one of the most intriguing new materials with extraordinary properties being discovered in the last decade. The unique structure of carbon nanotubes provides nanotubes with extraordinary mechanical and electrical properties. The outstanding properties that these materials possess have opened new interesting researches areas in nanoscience and nanotechnology. Although nanotubes are very promising in a wide variety of fields, application of individual nanotubes for large scale production has been limited. The main roadblocks, which hinder its use, are limited understanding of its synthesis and electrical properties which lead to difficulty in structure control, existence of impurities, and poor processability. This book makes an attempt to provide indepth study and analysis of various synthesis methods, processing techniques and characterization of carbon nanotubes that will lead to the increased applications of carbon nanotubes.

How to reference

In order to correctly reference this scholarly work, feel free to copy and paste the following:

I-Ling Chang (2011). Structural Instability of Carbon Nanotube, Carbon Nanotubes - Synthesis, Characterization, Applications, Dr. Siva Yellampalli (Ed.), ISBN: 978-953-307-497-9, InTech, Available from: <http://www.intechopen.com/books/carbon-nanotubes-synthesis-characterization-applications/structural-instability-of-carbon-nanotube>

INTECH
open science | open minds

InTech Europe

University Campus STeP Ri
Slavka Krautzeka 83/A
51000 Rijeka, Croatia
Phone: +385 (51) 770 447
Fax: +385 (51) 686 166
www.intechopen.com

InTech China

Unit 405, Office Block, Hotel Equatorial Shanghai
No.65, Yan An Road (West), Shanghai, 200040, China
中国上海市延安西路65号上海国际贵都大饭店办公楼405单元
Phone: +86-21-62489820
Fax: +86-21-62489821

© 2011 The Author(s). Licensee IntechOpen. This chapter is distributed under the terms of the [Creative Commons Attribution-NonCommercial-ShareAlike-3.0 License](#), which permits use, distribution and reproduction for non-commercial purposes, provided the original is properly cited and derivative works building on this content are distributed under the same license.

IntechOpen

IntechOpen